can be produced directly by the reduction of sintered oxides in a hydrogen atmosphere. This method has been used to obtains rods, discs and bars of various alloy compositions and shows promise as a means of preparation which avoids some of the existing problems in powder metallurgy.

References

1. J. S. HIRSCHHORN, "Introduction to Powder Metallurgy" (American Powder Metallurgy Institute, Princeton, NJ, 1969).
2. M. ROBBINS, M. L. GREEN, R. C. SHERWOOD, A. STAUDINGER and V. G. LAMBRECHT Jn., "Progress in Powder Metallurgy", Proceedings of the 1979 MPIF Meeting (submitted for publication).
3. M. L. GREEN, H. HERRING III, R. E. SHERWOOD, M. ROBBINS and V. G. LAMBRECHT Jn., *Int. J. Powder Met.* submitted for publication.
4. A. STAUDINGER, *J. Mater. Sci.* 15 (1980) 497.

Received 6 June
and accepted 29 August 1979.

M. ROBBINS
A. STAUDINGER
S. SHABAKA
Bell Laboratories,
Murray Hill, NJ 07974, USA

Observations of the reaction sintering of some β′-sialon compositions

The considerable interest in materials derived from the Al–Si–N–O system, and consisting principally of the β′-sialon phase ($Al_zSi_{6-z}N_{8-z}O_z$), arises in part because of their generally ready sinterability to full density. The early explanation suggested for the sintering behaviour of these materials was that vacant lattice sites enhanced atomic mobility [1]. However, it is now generally accepted that densification is the result of solution-reprecipitation processes involving oxygen-rich liquid phases at grain boundaries [2, 3]. Detailed attention has recently been paid to the solid–liquid equilibria existing in this system [4]. The importance of small amounts of liquid for the kinetics of reaction hot-pressing of β′-sialon materials has been noted [5], and it seems clear that compositions corresponding closely to β′-sialon itself will not densify, although important microstructural and chemical changes may occur [6]. These facts point to the likely importance of vapour phase or surface diffusion processes in this system at high temperature. We report here some results from studies of the reaction sintering behaviour of powder mixtures, corresponding to points spanning the β′-sialon phase line, at a *z* value in the region of 2, and which support conclusions drawn from the reaction hot-pressing studies.

The β′-sialon compositions are given in Table I, and are plotted on the $AlN–Al_2O_3–SiO_2–Si_3N_4$ diagram in Fig. 1. Contamination of the silicon nitride by silica (4 wt %) and the aluminium nitride by alumina (6 wt %) was allowed for. Powders were milled under propan-2-ol in an alumina charged polypropene vibro mill for 30 min. Corrections were also applied to take account of contamination of the powder by alumina (90 mg) during the milling process. Small pellets (10 mm long, 8 mm diameter, weighing ~ 800 mg) were pressed without binder at 200 MPa and embedded in either boron nitride powder or, more generally, one of a series of silicon nitride powders, in the cavity of a closed graphite crucible, and sintered

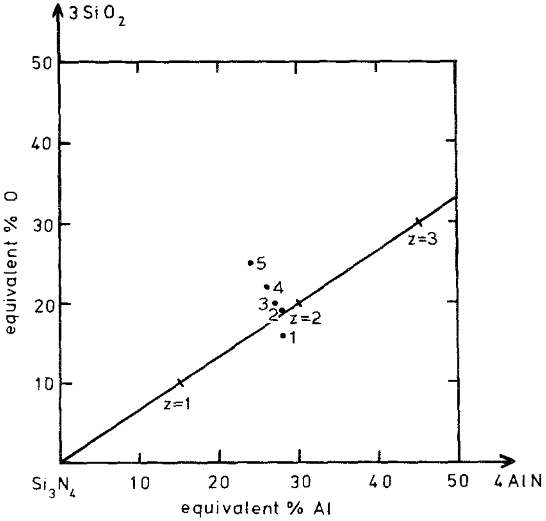

Figure 1 Points corresponding to the compositions studied, and their relationship to the β′-sialon phase line

TABLE I Compositions of materials studied

	Weights used (%)					
	AlN	Al_2O_3	Si_3N_4	Equivalent % O	Equivalent % Al	O/Al
1	15.9	18.3	65.8	16	28	0.58
2	13.1	20.6	66.3	19	28	0.69
3	11.1	21.9	67.0	20	27	0.73
4	6.7	24.8	68.5	22	26	0.86
5	1.2	28.8	70.0	25	24	1.05

for 1 h at 1800° C. Induction heating was used and the sintering temperature could be attained in 5 min from 1200° C. After cooling rapidly to room temperature the pellets were examined for weight and length changes. Qualitative X-ray diffraction analyses were carried out on powdered material to test for conversion of α-silicon nitride to β'-sialon. Fracture faces were also examined by scanning electron microscopy, and polished faces by optical microscopy.

Shrinkage and weight change data are shown in Fig. 2. The tendency for weight losses to occur is marked, and is related strongly to the nature of the powder bed used for the pellet. The smallest losses occurred when this was of the same silicon nitride powder as that used to form the pellet. The largest loss occurred when boron nitride was used. For compositions well above the β'-sialon line, the densification behaviour was inversely related to the weight loss, with densities approaching theoretical only being attainable when weight losses were less than 1%. For the composition below the β'-sialon line on the other hand, the opposite was true, and a weight loss appeared to be a prerequisite for significant densification. Shrinkage data, referred to conditions of zero weight loss, for the different β'-sialon compositions are plotted in Fig. 3. The β'-sialon composition is conveniently expressed in terms of the ratio [equivalent % O] / [equivalent % Al], the theoretical value of which for the β'-sialon phase is 0.67. Larger values indicate silica-rich material, and it is assumed that these also correspond to the presence of increasing amounts of liquid phase throughout the sintering process. The sensitivity of the system to slight departures from compositions corresponding to single-phase material is marked, and corresponds exactly to the behaviour observed under hot-pressing conditions. It is clear that in the absence of a permanent liquid phase, the densification rate is very slow indeed. X-ray diffraction examination of all sintered materials revealed, on the other hand, the disappearance of α-silicon nitride peaks, with the apparently complete formation of β'-sialon, even in materials where sintering shrinkage was insignificant. The scanning electron micrographs (Fig. 4) of composition 1 sintered under conditions of zero shrinkage also indicate that large scale microstructural rearrangement has occurred, with the formation of bridges between well developed crystallites. This feature is seen more clearly by optical micro-

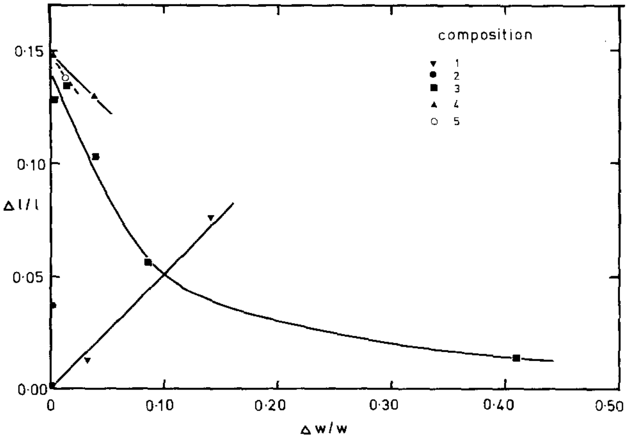

Figure 2 Isothermal shrinkage and weight loss data for a range of starting compositions, in different powder beds, after 1 h at 1800° C.

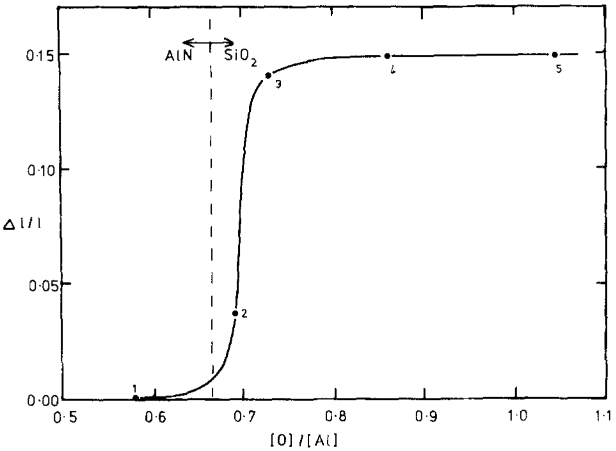

Figure 3 Isothermal shrinkages under conditions of zero weight loss, after 1 h at 1800° C, as a function of system composition expressed in terms of the [equivalent % oxygen]/[equivalent % aluminium] ratio.

scopy of polished sections (Fig. 5). At the same time reorganization, with agglomeration, of the fine-scale porosity has occurred.

It may be concluded that vapour phase and/or surface diffusion are likely to be important material transport processes in this system under the sintering conditions examined. These processes would permit the α-silicon nitride to β'-sialon reaction to take place, as well as the development of bridging neck regions between β'-sialon crystallites. In the absence of significant amounts of liquid phase to act as a vehicle for efficient Coble creep [7] in assisting the transport of material away from the grain-boundary regions, densification would then be effectively terminated. In this respect, therefore, the behaviour of the single-phase β'-sialon system appears to be that of a classical "unsinterable" covalent material [8] and special conditions, such as the use of ultra-fine powders, or additives able to generate liquid phases or suitably modify surface energy values, are required if appreciable densification is to occur.

It would appear, from the relationships observed between densification and weight loss in compositions above the β'-sialon line, that silicon monoxide is an important vapour-phase species. Its loss would deplete the system of the essential silica-rich grain-boundary phase, and impede the densification processes. It is of interest that direct observations of weight losses in the Al_2O_3–Si_3N_4 system [9] also point to the significance of silicon monoxide, as do detailed thermodynamic considerations [10]. The contrary behaviour of the powder with a composition below the β'-sialon line suggests that in this case aluminium nitride is preferentially lost to the surrounding silicon nitride bed. This would be possible through the dissociation:

$$AlN(c) \rightleftharpoons Al(g) + \tfrac{1}{2}N_2(g)$$

for which p_{Al} is of the order of 10^{-4} atm under a

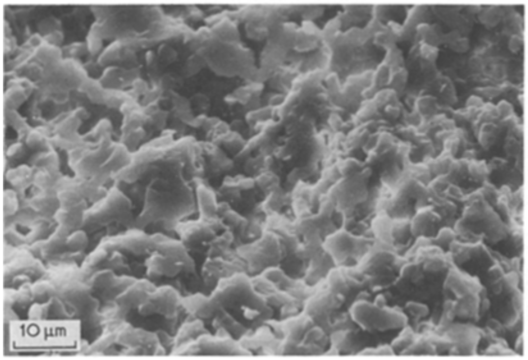

Figure 4 Fracture face of sample of composition 1 after sintering for 1 h at 1800° C.

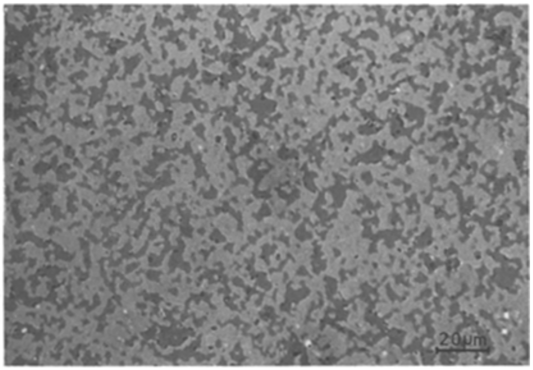

Figure 5 Polished section of sample of composition 1, after sintering for 1 h at 1800° C. Light regions, β'-sialon; dark regions, resin-filled porosity.

nitrogen partial pressure of ~ 1 atm, or 3×10^{-3} atm if a closed system is assumed. For a specific β'-sialon composition containing a glass phase, it is clear that there must be one optimum gaseous atmosphere, as defined by the silicon monoxide, nitrogen, aluminium vapour and silicon vapour partial pressures, if maximum densification is to be attained. For compositions containing initially an excess of aluminium nitride, and therefore no glass phase, densification is unlikely unless compositional changes occur, leading to the formation of grain-boundary glass.

Acknowledgement

The financial support of the Science Research Council in the form of a Research Grant, and a Research Studentship to M. Benn, is acknowledged.

References

1. K. H. JACK, *Trans. Brit. Ceram. Soc.* **72** (1973) 376.
2. *Idem, J. Mater. Sci.* **11** (1976) 1135.
3. M. H. LEWIS, B. D. POWELL, P. DREW, R. J. LUMBY, B. NORTH and A. J. TAYLOR, *ibid* **12** (1977) 61.
4. I. K. NAIK, L. J. GAUCKLER and T. Y. TIEN, *J. Amer. Ceram. Soc.* **61** (1978) 332.
5. M. BENN, M. KUWABARA and F. L. RILEY, "Science of Ceramics ', Vol. 9, edited by K. J. de Vries (Ned. Keramische Vereniging, Stoke-on-Trent, 1977) p. 119.
6. *Idem,* Proceedings of the International Symposium "Factors in Densification and Sintering of Oxide and Non-Oxide Ceramics", Hakone, 3–6 October 1978, edited by S. Saito (in press).
7. L. J. BOWEN, R. J. WESTON, T. G. CARRUTHERS and R. J. BROOK, *J. Mater. Sci.* **13** (1978) 341.
8. C. GRESKOVICH and J. H. ROSOLOWSKI, *J. Amer. Ceram. Soc.* **59** (1976) 336.
9. D. R. MESSIER and G. E. GAZZA, *ibid* **58** (1975) 538.
10. J. P. TORRE and A. MOCELLIN, in "Nitrogen Ceramics", edited by F. L. Riley, NATO Advanced Study Institute Applied Science Series No. 23 (Noordhoff, Leyden, 1977) p. 63.

Received 5 July
and accepted 27 July 1979

M. BENN
F. L. RILEY
Department of Ceramics,
University of Leeds,
Leeds, UK

Composite metallic glass wires

It is well documented that metallic glasses show an excellent high strength accompanying high ductility (capable of 180° bending without fracture) [1]. Focusing on such superior mechanical properties of metallic glasses, a reinforcement application has been of potential interest in practical use. For this purpose, the present study was conducted on a composite metallic glass wire (i.e. a conventional metal wire covered by a metallic glass) and its mechanical properties and fracture behaviour are reported.

$Fe_{78}Mo_2B_{20}$ metallic glass filaments were made by rapidly quenching from the molten alloy. The glassy nature of the resultant ribbon filaments, $48\,\mu m$ thick and 1.05 mm wide, was carefully examined using X-ray methods. In order to make a composite metallic glass wire, an as-quenched metallic glass ribbon was first drawn through diamond dies with reducing die diameters until it became virtually tube shaped. The detailed sequential observations of the cross-sectional change by drawing have been reported [2]. Then, a tip of a conventional metal wire, i.e. a wire reinforced by metallic glasses, was stuck into the groove of the metallic glass tube thus made. Subsequently, both the metal and metallic glass were simultaneously drawn through dies in multiple passes until the metallic glass material completely wrapped the conventional wire. A typical resultant composite wire thus made is shown in Fig. 1. The figure shows the optical micrograph of the cross-section of a copper composite metallic glass wire (inside and outside materials are copper and metallic glass, respectively). The surface of the cross-section as shown is mechanically polished. In a similar manner, an aluminium composite metallic glass wire was also made.

In order to evaluate their mechanical properties, the composite wires thus obtained were pulled to failure using an Instron tensile machine with a strain rate $\dot{\epsilon} = 4 \times 10^{-4}\,sec^{-1}$ at room temperature. In comparison to the stress–strain curves of a virgin as-quenched $Fe_{78}Mo_2B_{20}$ metallic glass ribbon, those of the composite

0022–2461/80/020532–3$02.30/0